

# Genuine Correlations of Like-Sign Particles in Hadronic $Z^0$ Decays

The OPAL Collaboration

## Abstract

Correlations among hadrons with the same electric charge produced in  $Z^0$  decays are studied using the high statistics data collected from 1991 through 1995 with the OPAL detector at LEP. Normalized factorial cumulants up to fourth order are used to measure genuine particle correlations as a function of the size of phase space domains in rapidity, azimuthal angle and transverse momentum. Both all-charge and like-sign particle combinations show strong positive genuine correlations. One-dimensional cumulants initially increase rapidly with decreasing size of the phase space cells but saturate quickly. In contrast, cumulants in two- and three-dimensional domains continue to increase. The strong rise of the cumulants for all-charge multiplets is increasingly driven by that of like-sign multiplets. This points to the likely influence of Bose-Einstein correlations. Some of the recently proposed algorithms to simulate Bose-Einstein effects, implemented in the Monte Carlo model PYTHIA, are found to reproduce reasonably well the measured second- and higher-order correlations between particles with the same charge as well as those in all-charge particle multiplets.

*To be submitted to Phys. Lett. B*

G. Abbiendi<sup>2</sup>, C. Ainsley<sup>5</sup>, P.F. Åkesson<sup>3</sup>, G. Alexander<sup>22</sup>, J. Allison<sup>16</sup>, G. Anagnostou<sup>1</sup>,  
 K.J. Anderson<sup>9</sup>, S. Arcelli<sup>17</sup>, S. Asai<sup>23</sup>, D. Axen<sup>27</sup>, G. Azuelos<sup>18,a</sup>, I. Bailey<sup>26</sup>, E. Barberio<sup>8</sup>,  
 R.J. Barlow<sup>16</sup>, R.J. Batley<sup>5</sup>, T. Behnke<sup>25</sup>, K.W. Bell<sup>20</sup>, P.J. Bell<sup>1</sup>, G. Bella<sup>22</sup>, A. Bellerive<sup>9</sup>,  
 G. Benelli<sup>4</sup>, S. Bethke<sup>32</sup>, O. Biebel<sup>32</sup>, I.J. Bloodworth<sup>1</sup>, O. Boeriu<sup>10</sup>, P. Bock<sup>11</sup>, J. Böhme<sup>25</sup>,  
 D. Bonacorsi<sup>2</sup>, M. Boutemour<sup>31</sup>, S. Braibant<sup>8</sup>, L. Brigliadori<sup>2</sup>, R.M. Brown<sup>20</sup>, H.J. Burckhart<sup>8</sup>,  
 J. Cammin<sup>3</sup>, R.K. Carnegie<sup>6</sup>, B. Caron<sup>28</sup>, A.A. Carter<sup>13</sup>, J.R. Carter<sup>5</sup>, C.Y. Chang<sup>17</sup>,  
 D.G. Charlton<sup>1,b</sup>, P.E.L. Clarke<sup>15</sup>, E. Clay<sup>15</sup>, I. Cohen<sup>22</sup>, J. Couchman<sup>15</sup>, A. Csilling<sup>8,i</sup>,  
 M. Cuffiani<sup>2</sup>, S. Dado<sup>21</sup>, G.M. Dallavalle<sup>2</sup>, S. Dallison<sup>16</sup>, A. De Roeck<sup>8</sup>, E.A. De Wolf<sup>8</sup>,  
 P. Dervan<sup>15</sup>, K. Desch<sup>25</sup>, B. Dienes<sup>30</sup>, M.S. Dixit<sup>6,a</sup>, M. Donkers<sup>6</sup>, J. Dubbert<sup>31</sup>, E. Duchovni<sup>24</sup>,  
 G. Duckeck<sup>31</sup>, I.P. Duerdoth<sup>16</sup>, E. Etzion<sup>22</sup>, F. Fabbri<sup>2</sup>, L. Feld<sup>10</sup>, P. Ferrari<sup>12</sup>, F. Fiedler<sup>8</sup>,  
 I. Fleck<sup>10</sup>, M. Ford<sup>5</sup>, A. Frey<sup>8</sup>, A. Fürtjes<sup>8</sup>, D.I. Futyan<sup>16</sup>, P. Gagnon<sup>12</sup>, J.W. Gary<sup>4</sup>,  
 G. Gaycken<sup>25</sup>, C. Geich-Gimbel<sup>3</sup>, G. Giacomelli<sup>2</sup>, P. Giacomelli<sup>2</sup>, D. Glenzinski<sup>9</sup>, J. Goldberg<sup>21</sup>,  
 K. Graham<sup>26</sup>, E. Gross<sup>24</sup>, J. Grunhaus<sup>22</sup>, M. Gruwé<sup>8</sup>, P.O. Günther<sup>3</sup>, A. Gupta<sup>9</sup>, C. Hajdu<sup>29</sup>,  
 M. Hamann<sup>25</sup>, G.G. Hanson<sup>12</sup>, K. Harder<sup>25</sup>, A. Harel<sup>21</sup>, M. Harin-Dirac<sup>4</sup>, M. Hauschild<sup>8</sup>,  
 J. Hauschildt<sup>25</sup>, C.M. Hawkes<sup>1</sup>, R. Hawkings<sup>8</sup>, R.J. Hemingway<sup>6</sup>, C. Hensel<sup>25</sup>, G. Herten<sup>10</sup>,  
 R.D. Heuer<sup>25</sup>, J.C. Hill<sup>5</sup>, K. Hoffman<sup>9</sup>, R.J. Homer<sup>1</sup>, D. Horváth<sup>29,c</sup>, K.R. Hossain<sup>28</sup>,  
 R. Howard<sup>27</sup>, P. Hütemeyer<sup>25</sup>, P. Igo-Kemenes<sup>11</sup>, K. Ishii<sup>23</sup>, A. Jawahery<sup>17</sup>, H. Jeremie<sup>18</sup>,  
 C.R. Jones<sup>5</sup>, P. Jovanovic<sup>1</sup>, T.R. Junk<sup>6</sup>, N. Kanaya<sup>26</sup>, J. Kanzaki<sup>23</sup>, G. Karapetian<sup>18</sup>,  
 D. Karlen<sup>6</sup>, V. Kartvelishvili<sup>16</sup>, K. Kawagoe<sup>23</sup>, T. Kawamoto<sup>23</sup>, R.K. Keeler<sup>26</sup>, R.G. Kellogg<sup>17</sup>,  
 B.W. Kennedy<sup>20</sup>, D.H. Kim<sup>19</sup>, K. Klein<sup>11</sup>, A. Klier<sup>24</sup>, S. Kluth<sup>32</sup>, T. Kobayashi<sup>23</sup>, M. Kobel<sup>3</sup>,  
 T.P. Kokott<sup>3</sup>, S. Komamiya<sup>23</sup>, R.V. Kowalewski<sup>26</sup>, T. Krämer<sup>25</sup>, T. Kress<sup>4</sup>, P. Krieger<sup>6</sup>, J. von  
 Krogh<sup>11</sup>, D. Krop<sup>12</sup>, T. Kuhl<sup>3</sup>, M. Kupper<sup>24</sup>, P. Kyberd<sup>13</sup>, G.D. Lafferty<sup>16</sup>, H. Landsman<sup>21</sup>,  
 D. Lanske<sup>14</sup>, I. Lawson<sup>26</sup>, J.G. Layter<sup>4</sup>, A. Leins<sup>31</sup>, D. Lellouch<sup>24</sup>, J. Letts<sup>12</sup>, L. Levinson<sup>24</sup>,  
 J. Lillich<sup>10</sup>, C. Littlewood<sup>5</sup>, S.L. Lloyd<sup>13</sup>, F.K. Loebinger<sup>16</sup>, G.D. Long<sup>26</sup>, M.J. Losty<sup>6,a</sup>, J. Lu<sup>27</sup>,  
 J. Ludwig<sup>10</sup>, A. Macchiolo<sup>18</sup>, A. Macpherson<sup>28,l</sup>, W. Mader<sup>3</sup>, S. Marcellini<sup>2</sup>, T.E. Marchant<sup>16</sup>,  
 A.J. Martin<sup>13</sup>, J.P. Martin<sup>18</sup>, G. Martinez<sup>17</sup>, G. Masetti<sup>2</sup>, T. Mashimo<sup>23</sup>, P. Mättig<sup>24</sup>,  
 W.J. McDonald<sup>28</sup>, J. McKenna<sup>27</sup>, T.J. McMahon<sup>1</sup>, R.A. McPherson<sup>26</sup>, F. Meijers<sup>8</sup>,  
 P. Mendez-Lorenzo<sup>31</sup>, W. Menges<sup>25</sup>, F.S. Merritt<sup>9</sup>, H. Mes<sup>6,a</sup>, A. Michelini<sup>2</sup>, S. Mihara<sup>23</sup>,  
 G. Mikenberg<sup>24</sup>, D.J. Miller<sup>15</sup>, S. Moed<sup>21</sup>, W. Mohr<sup>10</sup>, T. Mori<sup>23</sup>, A. Mutter<sup>10</sup>, K. Nagai<sup>13</sup>,  
 I. Nakamura<sup>23</sup>, H.A. Neal<sup>33</sup>, R. Nisius<sup>8</sup>, S.W. O’Neale<sup>1</sup>, A. Oh<sup>8</sup>, A. Okpara<sup>11</sup>, M.J. Oreglia<sup>9</sup>,  
 S. Orito<sup>23</sup>, C. Pahl<sup>32</sup>, G. Pásztor<sup>8,i</sup>, J.R. Pater<sup>16</sup>, G.N. Patrick<sup>20</sup>, J.E. Pilcher<sup>9</sup>, J. Pinfold<sup>28</sup>,  
 D.E. Plane<sup>8</sup>, B. Poli<sup>2</sup>, J. Polok<sup>8</sup>, O. Pooth<sup>8</sup>, A. Quadt<sup>3</sup>, K. Rabbertz<sup>8</sup>, C. Rembser<sup>8</sup>, P. Renkel<sup>24</sup>,  
 H. Rick<sup>4</sup>, N. Rodning<sup>28</sup>, J.M. Roney<sup>26</sup>, S. Rosati<sup>3</sup>, K. Roscoe<sup>16</sup>, Y. Rozen<sup>21</sup>, K. Runge<sup>10</sup>,  
 D.R. Rust<sup>12</sup>, K. Sachs<sup>6</sup>, T. Saeki<sup>23</sup>, O. Sahr<sup>31</sup>, E.K.G. Sarkisyan<sup>8,m</sup>, C. Sbarra<sup>26</sup>, A.D. Schaile<sup>31</sup>,  
 O. Schaile<sup>31</sup>, P. Scharff-Hansen<sup>8</sup>, M. Schröder<sup>8</sup>, M. Schumacher<sup>25</sup>, C. Schwick<sup>8</sup>, W.G. Scott<sup>20</sup>,  
 R. Seuster<sup>14,g</sup>, T.G. Shears<sup>8,j</sup>, B.C. Shen<sup>4</sup>, C.H. Shepherd-Themistocleous<sup>5</sup>, P. Sherwood<sup>15</sup>,  
 A. Skuja<sup>17</sup>, A.M. Smith<sup>8</sup>, G.A. Snow<sup>17</sup>, R. Sobie<sup>26</sup>, S. Söldner-Rembold<sup>10,e</sup>, S. Spagnolo<sup>20</sup>,  
 F. Spano<sup>9</sup>, M. Sproston<sup>20</sup>, A. Stahl<sup>3</sup>, K. Stephens<sup>16</sup>, D. Strom<sup>19</sup>, R. Ströhmer<sup>31</sup>, L. Stumpf<sup>26</sup>,  
 B. Surrow<sup>25</sup>, S. Tarem<sup>21</sup>, M. Tasevsky<sup>8</sup>, R.J. Taylor<sup>15</sup>, R. Teuscher<sup>9</sup>, J. Thomas<sup>15</sup>,  
 M.A. Thomson<sup>5</sup>, E. Torrence<sup>19</sup>, D. Toya<sup>23</sup>, T. Trefzger<sup>31</sup>, A. Tricoli<sup>2</sup>, I. Trigger<sup>8</sup>,  
 Z. Trócsányi<sup>30,f</sup>, E. Tsur<sup>22</sup>, M.F. Turner-Watson<sup>1</sup>, I. Ueda<sup>23</sup>, B. Ujvári<sup>30,f</sup>, B. Vachon<sup>26</sup>,  
 C.F. Vollmer<sup>31</sup>, P. Vannerem<sup>10</sup>, M. Verzocchi<sup>17</sup>, H. Voss<sup>8</sup>, J. Vossebeld<sup>8</sup>, D. Waller<sup>6</sup>, C.P. Ward<sup>5</sup>,  
 D.R. Ward<sup>5</sup>, P.M. Watkins<sup>1</sup>, A.T. Watson<sup>1</sup>, N.K. Watson<sup>1</sup>, P.S. Wells<sup>8</sup>, T. Wengler<sup>8</sup>,  
 N. Wormes<sup>3</sup>, D. Wetterling<sup>11</sup>, G.W. Wilson<sup>16</sup>, J.A. Wilson<sup>1</sup>, T.R. Wyatt<sup>16</sup>, S. Yamashita<sup>23</sup>,  
 V. Zacek<sup>18</sup>, D. Zer-Zion<sup>8,k</sup>

- <sup>1</sup>School of Physics and Astronomy, University of Birmingham, Birmingham B15 2TT, UK
- <sup>2</sup>Dipartimento di Fisica dell' Università di Bologna and INFN, I-40126 Bologna, Italy
- <sup>3</sup>Physikalisches Institut, Universität Bonn, D-53115 Bonn, Germany
- <sup>4</sup>Department of Physics, University of California, Riverside CA 92521, USA
- <sup>5</sup>Cavendish Laboratory, Cambridge CB3 0HE, UK
- <sup>6</sup>Ottawa-Carleton Institute for Physics, Department of Physics, Carleton University, Ottawa, Ontario K1S 5B6, Canada
- <sup>8</sup>CERN, European Organisation for Nuclear Research, CH-1211 Geneva 23, Switzerland
- <sup>9</sup>Enrico Fermi Institute and Department of Physics, University of Chicago, Chicago IL 60637, USA
- <sup>10</sup>Fakultät für Physik, Albert Ludwigs Universität, D-79104 Freiburg, Germany
- <sup>11</sup>Physikalisches Institut, Universität Heidelberg, D-69120 Heidelberg, Germany
- <sup>12</sup>Indiana University, Department of Physics, Swain Hall West 117, Bloomington IN 47405, USA
- <sup>13</sup>Queen Mary and Westfield College, University of London, London E1 4NS, UK
- <sup>14</sup>Technische Hochschule Aachen, III Physikalisches Institut, Sommerfeldstrasse 26-28, D-52056 Aachen, Germany
- <sup>15</sup>University College London, London WC1E 6BT, UK
- <sup>16</sup>Department of Physics, Schuster Laboratory, The University, Manchester M13 9PL, UK
- <sup>17</sup>Department of Physics, University of Maryland, College Park, MD 20742, USA
- <sup>18</sup>Laboratoire de Physique Nucléaire, Université de Montréal, Montréal, Quebec H3C 3J7, Canada
- <sup>19</sup>University of Oregon, Department of Physics, Eugene OR 97403, USA
- <sup>20</sup>CLRC Rutherford Appleton Laboratory, Chilton, Didcot, Oxfordshire OX11 0QX, UK
- <sup>21</sup>Department of Physics, Technion-Israel Institute of Technology, Haifa 32000, Israel
- <sup>22</sup>Department of Physics and Astronomy, Tel Aviv University, Tel Aviv 69978, Israel
- <sup>23</sup>International Centre for Elementary Particle Physics and Department of Physics, University of Tokyo, Tokyo 113-0033, and Kobe University, Kobe 657-8501, Japan
- <sup>24</sup>Particle Physics Department, Weizmann Institute of Science, Rehovot 76100, Israel
- <sup>25</sup>Universität Hamburg/DESY, II Institut für Experimental Physik, Notkestrasse 85, D-22607 Hamburg, Germany
- <sup>26</sup>University of Victoria, Department of Physics, P O Box 3055, Victoria BC V8W 3P6, Canada
- <sup>27</sup>University of British Columbia, Department of Physics, Vancouver BC V6T 1Z1, Canada
- <sup>28</sup>University of Alberta, Department of Physics, Edmonton AB T6G 2J1, Canada
- <sup>29</sup>Research Institute for Particle and Nuclear Physics, H-1525 Budapest, P O Box 49, Hungary
- <sup>30</sup>Institute of Nuclear Research, H-4001 Debrecen, P O Box 51, Hungary
- <sup>31</sup>Ludwigs-Maximilians-Universität München, Sektion Physik, Am Coulombwall 1, D-85748 Garching, Germany
- <sup>32</sup>Max-Planck-Institute für Physik, Föhring Ring 6, 80805 München, Germany
- <sup>33</sup>Yale University, Department of Physics, New Haven, CT 06520, USA

<sup>a</sup> and at TRIUMF, Vancouver, Canada V6T 2A3

<sup>b</sup> and Royal Society University Research Fellow

<sup>c</sup> and Institute of Nuclear Research, Debrecen, Hungary

<sup>e</sup> and Heisenberg Fellow

<sup>f</sup> and Department of Experimental Physics, Lajos Kossuth University, Debrecen, Hungary

<sup>g</sup> and MPI München

<sup>i</sup> and Research Institute for Particle and Nuclear Physics, Budapest, Hungary

<sup>j</sup> now at University of Liverpool, Dept of Physics, Liverpool L69 3BX, UK

<sup>k</sup> and University of California, Riverside, High Energy Physics Group, CA 92521, USA

<sup>l</sup> and CERN, EP Div, 1211 Geneva 23

<sup>m</sup> and Tel Aviv University, School of Physics and Astronomy, Tel Aviv 69978, Israel.

# 1 Introduction

Correlations in momentum space between hadrons produced in high energy interactions have been extensively studied over many decades in different contexts [1]. Being a measure of event-to-event fluctuations of the number of hadrons in a phase space domain of size  $\Delta$ , correlations provide detailed information on the hadronisation dynamics, complementary to that derived from inclusive single-particle distributions and global event-shape characteristics.

The suggestion in [2] that multiparticle dynamics might possess (multi-)fractal properties or be “intermittent”, emphasized the importance of studying correlations as a function of the size of domains in momentum space. A key ingredient for such studies is the normalized factorial moment and factorial cumulant technique (see Sect. 2), which allows statistically meaningful results to be obtained even for very small phase space cells.

Unlike factorial moments, cumulants of order  $q$  are a direct measure of the stochastic interdependence among groups of exactly  $q$  particles emitted in the same phase space cell [3–5]. Therefore, they are well suited for the study of true or “genuine” correlations between hadrons.

Whereas earlier work dealt mainly with correlations between pairs *i.e.* *second-order* correlations, the use of factorial cumulants in high-statistics experiments has established the presence of genuine correlations among groups comprising three or more hadrons, hereafter referred to as *higher-order* correlations.

Experimental results on hadron correlations are reviewed in [1,6]. Except for heavy ion collisions, where correlations beyond second order are found to be small, as can be understood from a superposition of independent particle-production sources [7], in all other types of reactions, significant positive higher-order correlations are seen. In two- or three-dimensional (typically rapidity, azimuthal angle, transverse momentum) phase space cells, they rapidly increase as the cell-size,  $\Delta$ , becomes smaller. Further studies of the dependence on particle charge confirm that, as conjectured in [8], correlations between hadrons with the same charge play an increasingly important role as  $\Delta$  decreases, thus pointing to the influence of Bose-Einstein (BE) interference effects [9,10]; for a recent review see [11]. In contrast, correlations in multiplets composed of particles with different charges, which are more sensitive to multiparticle resonance decays than like-sign ones, tend to saturate in small phase space domains [12,13].

Two-particle Bose-Einstein correlations (BEC) have been observed in a wide range of multihadronic processes [11]. Such correlations were extensively studied at LEP [14–16]. Evidence for BEC among groups of more than two identical particles has also been reported [13,17]. The subject has acquired particular importance in connection with high-precision measurements of the  $W$ -boson mass at LEP-II [18,19]. For these, better knowledge of correlations in general is needed, as well as realistic Monte Carlo modelling of BEC [20,21].

The OPAL collaboration recently reported an analysis of the domain-size dependence of factorial cumulants in hadronic  $Z^0$  decays, using much larger statistics than in any previous experiment [22]. In that study, no distinction was made between multiplets composed of like-charge particles and those of mixed charge. Clear evidence was seen for large positive genuine correlations up to fifth order. Hard jet production was found to contribute significantly to the observed particle fluctuation patterns. However, Monte Carlo models based on parton showers and string or cluster fragmentation, gave only a qualitative description of the  $\Delta$ -dependence of the cumulants. Quantitatively, the model studied, which did not explicitly include BE-type correlation effects, underestimated significantly correlations between hadrons produced very

close together in momentum space.

In the present paper, the high statistics OPAL data collected at and near the  $Z^0$  centre-of-mass energy are used to measure cumulants for multiplets of particles with the same charge, hereafter referred to as “like-sign cumulants”. They are compared to “all-charge” cumulants, corresponding to multiplets comprising particles of any (positive or negative) charge. Using the factorial cumulant technique, results of much higher precision than previously available are obtained on like-sign correlations up to fourth order. The role of Bose-Einstein-type effects is studied, using recently proposed BEC algorithms<sup>1</sup> in the Monte Carlo event generator PYTHIA for  $e^+e^-$  annihilation [24]. Proceeding beyond the usual analyses of two-particle correlations, we show that, at least within the framework of this model, a good description can be achieved of the factorial cumulants up to fourth order in one-, two- and three-dimensional phase space domains.

The paper is organized as follows. Section 2 explains the normalized factorial cumulant method which allows genuine particle correlations to be measured. The OPAL detector, the event selection and the track selection criteria are detailed in Sect. 3. The data on factorial cumulants are presented in Sect. 4. They are compared with PYTHIA predictions and, in particular, with several variants of a model to simulate the Bose-Einstein effect. The results are summarized in Sect. 5. A brief overview of some of the BEC algorithms implemented in PYTHIA is given in the appendix.

## 2 Factorial cumulant method

To measure genuine multiparticle correlations in multi-dimensional phase space cells, we use the technique of normalized factorial cumulant moments,  $K_q$ , or “cumulants” for brevity, as proposed in [5].

In the present paper, the cumulants are computed as in a previous OPAL analysis [22]. A  $D$ -dimensional region of phase space (defined in Sect. 3) is partitioned into  $M^D$  cells of equal size  $\Delta$ . From the number of particles counted in each cell,  $n_m$  ( $m = 1, \dots, M^D$ ), event-averaged unnormalized factorial moments,  $\langle n_m^{[q]} \rangle$ , and unnormalized cumulants,  $k_q^{(m)}$ , are derived, using the relations given e.g. in [3]. For  $q = 2, 3, 4$ , one has

$$k_2^{(m)} = \langle n_m^{[2]} \rangle - \langle n_m \rangle^2, \quad (1)$$

$$k_3^{(m)} = \langle n_m^{[3]} \rangle - 3 \langle n_m^{[2]} \rangle \langle n_m \rangle + 2 \langle n_m \rangle^3 \quad (2)$$

$$k_4^{(m)} = \langle n_m^{[4]} \rangle - 4 \langle n_m^{[3]} \rangle \langle n_m \rangle - 3 \langle n_m^{[2]} \rangle^2 + 12 \langle n_m^{[2]} \rangle \langle n_m \rangle^2 - 6 \langle n_m \rangle^4. \quad (3)$$

Here,  $\langle n^{[q]} \rangle = \langle n(n-1)\dots(n-q+1) \rangle$  and the brackets  $\langle \cdot \rangle$  indicate that the average over all events is taken.

Normalized cumulants are calculated using the expression

$$K_q = (\mathcal{N})^q \overline{k_q^{(m)}} / \overline{N_m^{[q]}}. \quad (4)$$

---

<sup>1</sup>A variety of methods which try to simulate BE-effects in Monte Carlo generators have been developed. A detailed exposition of the basic physics issues involved and a review of the presently most popular models and algorithms can be found in [23].

As proposed in [25], this form is used to correct for statistical bias and non-uniformity of the single-particle spectra. Here,  $N_m$  is the number of particles in the  $m$ th cell summed over all  $\mathcal{N}$  events in the sample,  $N_m = \sum_{j=1}^{\mathcal{N}} (n_m)_j$ . The horizontal bar indicates averaging over the  $M^D$  cells in each event,  $(1/M^D) \sum_{m=1}^{M^D}$ .

The factorial moment of order  $q$  of the multiplicity distribution of particles *of the same species* (e.g. all charged, negatives only, ...) in a phase space domain  $\Delta$  is equal to the integral of the  $q$ -particle inclusive density,  $\rho_q$ , over that domain [1]. As in the cluster expansion in statistical mechanics,  $\rho_q$  can be decomposed into the sum of contributions from “accidental” coincidences of particles in  $\Delta$  and the true or “genuine” correlations. The latter are denoted here by the unnormalised cumulants,  $k_q$ , being the bin-averaged factorial cumulant functions, or “correlation functions”, for short [4].

Whereas  $\langle n^{[q]} \rangle$  depends on all correlation functions of order  $1 \leq p \leq q$ ,  $k_q$  is a direct measure of stochastic dependence in multiplets of exactly  $q$  particles. By construction,  $k_q$  vanishes whenever a particle within the  $q$ -tuple is statistically independent of one of the others. For Poissonian multiplicity fluctuations, the cumulants of all orders  $q > 1$  vanish identically. Non-zero cumulants therefore signal the presence of correlations.

In the following, data are presented for “all-charge” and for “like-sign” multiplets. For the former, the cell-counts  $n_m$  are determined using all charged particles in an event, irrespective of their charge. For the latter, the number of positive particles and the number of negative particles in a cell are counted separately. The corresponding cumulants are then averaged to obtain those for like-sign multiplets. It is to be noted that the cell-counting technique does not allow correlations to be measured directly among groups composed of particles of different charge. For these, other methods, such as correlation integrals (see e.g. Sect. 4.8 in [1]) have to be used. Nevertheless, cumulants for unlike-sign pairs can be indirectly derived using the equation

$$K_2^{\text{all}} = \frac{1}{2} K_2^{\text{ls}} + \frac{1}{2} K_2^{\text{us}}, \quad (5)$$

which relates second-order cumulants for all-charge pairs to those of like-sign (ls) and unlike-sign (us) pairs.

### 3 Experimental details

The present analysis uses a sample of approximately  $4.1 \times 10^6$  hadronic  $Z^0$  decays collected from 1991 through 1995. About 91% of this sample was taken at the  $Z^0$ ; the remaining part has a centre-of-mass energy,  $\sqrt{s}$ , within  $\pm 3$  GeV of the  $Z^0$  peak.

The OPAL detector has been described in detail in [26]. The results presented here are mainly based on the information from the central tracking chambers, which consist of a silicon microvertex detector, a vertex chamber, a jet chamber with 24 sectors each containing 159 axial anode wires, and outer  $z$ -chambers to improve the  $z$  coordinate resolution<sup>2</sup>. These detectors

---

<sup>2</sup>The right-handed OPAL coordinate system is defined with the  $z$  axis pointing in the direction of the  $e^-$  beam and the  $x$  axis pointing towards the centre of the LEP ring.  $r$  is the coordinate normal to the beam axis,  $\varphi$  the azimuthal angle with respect to the  $x$  axis,  $\theta$  the polar angle with respect to the  $z$ -axis.



are located in a 0.435 T axial magnetic field and measure  $p_t$ , the track momentum transverse to the beam axis, with a precision of  $(\sigma_{p_t}/p_t) = \sqrt{(0.02)^2 + (0.0015 p_t)^2}$  ( $p_t$  in GeV/c) for  $|\cos\theta| < 0.73$ . The jet chamber also measures the specific energy loss of charged particles,  $dE/dx$ , with a resolution  $\sigma(dE/dx)/(dE/dx) \simeq 3.5\%$  for a track having 159 hits in the jet chamber. The energy loss is used to identify charged particles [27].

A sample of over 2 million events was generated with JETSET 7.4/PYTHIA6.1 [24], including a full simulation of the detector [28]. The model parameters were previously tuned to OPAL data [29, 30] but Bose-Einstein effects were not explicitly incorporated. These events were used to determine the efficiencies of track and event selection and for correction purposes. In addition, for the evaluation of systematic errors, over 1.1 million events were simulated with PYTHIA including BEC with the algorithm<sup>3</sup> BE<sub>32</sub>.

The event selection criteria are based on the multihadronic event selection algorithms described in [22]. It was required that tracks have at least 20 hits in the jet chamber, a first measured point at a maximum radial distance from the interaction point of 70 cm, a minimum transverse momentum with respect to the beam direction,  $p_t$ , of 0.15 GeV/c, a measured momentum  $p$  smaller than 10 GeV/c, a measured polar angle satisfying  $|\cos\theta| < 0.93$ , and a measured distance of closest approach to the origin of less than 5 cm in the  $r - \varphi$  plane, and less than 40 cm in the  $z$  direction.

The mean energy loss,  $dE/dx$ , of a track was required to be less than 9 keV/cm, thereby rejecting electrons and positrons. About 97% of photon conversion pairs were rejected, reducing the conversion background in the sample to less than 0.1% of the number of tracks [27]. The fraction of pions in the track sample was estimated from Monte Carlo simulation to be about 80%.

Selected multihadron events were required to have at least 5 good tracks, a momentum imbalance (the magnitude of the vector sum of the momenta of all charged particles) of less than  $0.4 \sqrt{s}$  and the sum of the energies of all tracks (assumed to be pions) greater than  $0.2 \sqrt{s}$ . These requirements provide rejection of background from non-hadronic  $Z^0$  decays, two-photon events, beam-wall and beam-gas interactions. In addition, the polar angle of the event sphericity axis, calculated using tracks that passed the above cuts, as well as unassociated electromagnetic and hadronic calorimeter clusters, had to satisfy  $|\cos\theta_{\text{sph}}| < 0.7$  in order to accept only events well contained in the detector. A total of about  $2.3 \times 10^6$  events were finally selected for further analysis.

The cumulant analysis is performed in the kinematic variables rapidity,  $y$ , azimuthal angle,  $\Phi$ , and the transverse momentum variable,  $\ln p_T$ , all calculated with respect to the sphericity axis.

- Rapidity is defined as  $y = 0.5 \ln[(E + p_{\parallel})/(E - p_{\parallel})]$ , with  $E$  and  $p_{\parallel}$  the energy (assuming the pion mass) and longitudinal momentum of the particle, respectively. Only particles within the central rapidity region  $-2.0 \leq y \leq 2.0$  were retained.
- In transverse momentum subspace, the logarithm of  $p_T$ , instead of  $p_T$  itself, is used to eliminate as much as possible the strong dependence of the cumulants on cell-size arising

---

<sup>3</sup>We used algorithm BE<sub>32</sub> (see [23] and the appendix) in subroutine PYBOEI with parameters MSTJ(51)=2, MSTJ(52)=9, PARJ(92)=1.0, PARJ(93)=0.5 GeV. PARJ(92) is equal to  $\lambda$  in Eqs. (8) and (9) of the appendix; the parameter  $R$  is given by  $\hbar c/\text{PARJ}(93)$ .



from the nearly exponential shape of the  $p_T^2$ -distribution. Only particles within the range  $-2.4 \leq \ln(p_T) \leq 0.7$  ( $p_T$  in GeV/ $c$ ) were used.

- The azimuthal angle,  $\Phi$ , is calculated with respect to the eigenvector of the momentum tensor having the smallest eigenvalue in the plane perpendicular to the sphericity axis. The angle  $\Phi$  spans the interval  $0 \leq \Phi < 2\pi$ .

The phase space is partitioned into  $M$  bins of equal size for each of the three variables.  $M$  varies between 1 (full interval) and 400, corresponding to a smallest bin size in one dimension of  $\delta y_{\min} = 0.01$ ,  $\delta\Phi_{\min} = 0.9^\circ$  and  $\delta(\ln p_T)_{\min} = 0.008$ , each significantly larger than the experimental resolution of the OPAL detector.

The cumulants for like-sign and all-charge multiplts, measured as a function of  $M$ , have been corrected for geometrical acceptance, kinematic cuts, initial-state radiation, resolution, secondary interactions and decays in the detector, using correction factors,  $U_q(M)$ , calculated for all-charge particle combinations and evaluated as in [22] using the JETSET/PYTHIA Monte Carlo without BEC.

As systematic uncertainties, we include the following contributions:

- The statistical error of the correction factors  $U_q(M)$ . Statistical errors due to the finite statistics of the Monte Carlo samples are comparable to those of the data.
- Track and event selection criteria variations as in [22]. To this end, the cumulants have been computed changing in turn the following selection criteria: the first measured point was required to be closer than 40 cm to the beam, the requirement of the transverse momentum with respect to the beam axis was removed, the momentum was required to be less than 40 GeV/ $c$ , the track polar angle acceptance was changed to  $|\cos\theta| < 0.7$ , and the requirement on the mean energy loss was removed. These changes modify the results by no more than a few percent in the smallest cells, and do not affect the conclusions.
- The difference between cumulants corrected with the factors  $U_q(M)$  derived from Monte-Carlo calculations with and without Bose-Einstein simulation. The correction factors in these two cases differ by at most 5% in the smallest bins.
- The difference between cumulants corrected with  $U_q(M)$ -factors, calculated for all-charge particle combinations and those calculated for like-sign combinations. The correction factors coincide within 1%.

The total errors have been calculated by adding the systematic and statistical uncertainties in quadrature. It was further verified that our conclusions remain unchanged when events taken at energies off the  $Z^0$  peak are excluded from the analysis.

## 4 Results

### 4.1 Like-sign and all-charge cumulants

The fully corrected normalized cumulants  $K_q$  ( $q = 2, 3, 4$ ) for all-charge<sup>4</sup> and like-sign particle multiplets, calculated in one-dimensional ( $y$  and  $\Phi$ ) (1D), two-dimensional  $y \times \Phi$  (2D) and three-dimensional  $y \times \Phi \times \ln p_T$  (3D) phase space cells, are displayed in Fig. 1 and Fig. 2.

From Fig. 1 it is seen that, even in 1D, positive genuine correlations among groups of two, three and four particles are present:  $K_q > 0$ . They are substantially stronger in rapidity than in azimuthal angle. The cumulants increase rapidly with increasing  $M$ , the inverse of the bin size, for relatively large domains but saturate rather quickly. For  $K_2$  this behaviour follows from the shape of the second-order correlation function which is known to be approximately Gaussian [1] in the two-particle rapidity difference  $\Delta \equiv \delta y$ . The rapid rise and subsequent saturation can be understood from hard gluon jet emission. For small  $M$ , the cumulants are sensitive to the large-scale structure of the event, where any jet non-collinear with the event axis produces a strong fluctuation in the particle density. With  $M$  increasing, the structure inside a single jet is progressively probed.

In contrast to 1D cumulants, those in 2D and 3D (Fig. 2) continue to increase towards small phase space cells. Moreover, the 2D and 3D cumulants are of similar magnitude at fixed  $M$ , indicating that the contribution from correlations in transverse momentum is small. This can be understood from the importance of multi-jet production in  $e^+e^-$  annihilation, which is most prominently observed in  $y \times \Phi$  space [22]. Indeed, the 1D cumulants in  $p_T$  are found to be close to zero and therefore not shown.

It is to be noted that oscillations of the cumulants, clearly seen in the data as well as in the Monte Carlo predictions (see *e.g.*  $K_q(\Phi)$  in Fig. 1) are not due to statistical fluctuations. They arise from the jet structure of the events in rapidity-azimuthal angle subspace, and from the phase space partitioning technique used to calculate the cumulants as a function of  $M$ .

The 1D cumulants of all-charge and of like-sign multiplets (Fig. 1) show a similar dependence on  $M$ . The latter, however, are significantly smaller, implying that, for all  $M$ , correlations among particles of opposite charge are important in one-dimensional phase space projections. Using Eq. (5), it is found *e.g.* that the one-dimensional cumulants for unlike-charge pairs are larger by a factor of 1.6–1.7 than those of like-sign pairs for  $M \gtrsim 5$ . This can be expected in general from local charge conservation and in particular from resonance decays.

In 2D and 3D (Fig. 2), like-sign cumulants increase faster and approach the all-charge ones at large  $M$ . From Eq. (5), it can be inferred that  $K_2$  for unlike-charge pairs remains essentially constant for  $M$  larger than about 6. Consequently, as the cell-size becomes smaller, the rise of all-charge correlations is increasingly driven by that of like-sign multiplets.

Similar features, but based on measurements of *factorial moments*, were observed in other experiments [12] and, mainly on qualitative grounds, taken as evidence for the large influence of the Bose-Einstein effect on all-charge correlations in small phase space domains<sup>5</sup>. In the next section, we add quantitative support to those earlier observations, showing that algorithms which simulate BEC indeed allow a quite successful description of the measurements.

---

<sup>4</sup>The data points for all-charge particle combinations are the same as those published in [22] but include different systematic uncertainties.

<sup>5</sup>For a recent critical review we refer to [31].

## 4.2 Model comparison

In this section, we compare the cumulant data with predictions of the PYTHIA Monte Carlo event generator (version 6.158) without and with Bose-Einstein effects. Samples of about  $10^6$  multihadronic events were generated at the  $Z^0$  energy. The model parameters, not related to BEC, were set at values obtained from a previous tune to OPAL data on event-shape and single-particle inclusive distributions [29]. In this tuning, BE-effects were not included.

To assess the importance of BE-type short-range correlations between identical particles, and their influence on all-charge cumulants, we concentrate on the algorithm BE<sub>32</sub>, described in the appendix, using parameter values  $\text{PARJ}(93) = 0.26$  GeV ( $R = 0.76$  fm) and  $\text{PARJ}(92) \equiv \lambda = 1.5$ . These values were determined by varying independently  $\text{PARJ}(93)$  and  $\lambda$  within the range 0.2–0.5 GeV and 0.5–2.2, respectively, in steps of 0.05 GeV and 0.1, leaving all other model-parameters unchanged, until satisfactory agreement with the measured cumulants  $K_2$  for like-sign pairs was reached<sup>6</sup>. Whereas a detailed multi-dimensional best-fit tuning procedure was considered to be outside the scope of the paper, we find that calculations with  $\text{PARJ}(93)$  in the range 0.2 – 0.3 GeV, and the corresponding  $\lambda$  in the range 1.7 – 1.3, still provide an acceptable description of the second-order like-sign cumulants.

Additional studies have revealed some sensitivity of single-particle spectra and event shapes to the inclusion of BEC in PYTHIA. Nevertheless, it was found that minor variations of the QCD and fragmentation parameters are sufficient to restore agreement with these data, while the changes in the predicted cumulants remain well within the systematic uncertainties of the measurement. These parameters were, therefore, not changed from their values listed in footnote 6.

The dashed lines in Figs. 1 and 2 show PYTHIA predictions for *like-sign* multiplets for the model without BEC. Model and data agree for small  $M$  (large phase space domains), indicating that the multiplicity distribution in those regions is well modelled. However, for larger  $M$ , the predicted cumulants are too small, the largest deviations occurring in 2D and 3D. The model predicts negative values for  $K_4(\Phi)$  which are not shown.

The solid curves in Figs. 1 and 2 show predictions for *like-sign* multiplets using the BE<sub>32</sub> algorithm. Inclusion of BEC leads to a very significant improvement of the data description. Not only two-particle but also higher order correlations in 1D rapidity space are well accounted for. In  $\Phi$ -space (Fig. 1),  $K_3$  and especially (the very small)  $K_4$  are less well reproduced. Figure 2 also shows that the predicted 2D and 3D cumulants agree well with the data.

For more clarity and later reference, the 1D, 2D and 3D cumulants for particle pairs with the same charge are repeated in Fig. 3. Since BEC occur only when two identical mesons are close-by in all three phase space dimensions, projection onto lower-dimensional subspaces, such as rapidity and azimuthal angle, leads to considerable weakening of the effect. Nevertheless, the high precision of the data in Fig. 3 allows to demonstrate clear sensitivity to the presence or absence of BEC in the model, which was much less evident in earlier measurements [1].

Whereas the BE-algorithm used implements pair-wise BEC only, it is noteworthy that the procedure also induces like-sign higher-order correlations of approximately correct magnitude. This seems to indicate that high-order cumulants are, to a large extent, determined by the second-order one (see further Sect. 4.3). It is not clear, however, whether the agreement is acci-

---

<sup>6</sup>Non-BEC related model-parameters were set at the following values:  $\text{PARJ}(21)=0.4$  GeV,  $\text{PARJ}(42)=0.52$  GeV<sup>-2</sup>,  $\text{PARJ}(81)=0.25$  GeV,  $\text{PARJ}(82)=1.9$  GeV.

dental or implies that the physics of  $n$ -boson ( $n > 2$ ) BE effects is indeed correctly simulated<sup>7</sup>.

The influence of like-sign BE-type correlations on the correlations in all-charge multiplets becomes clear from Figs. 4 and 5 where all-charge cumulants are compared with PYTHIA predictions without BEC, and for various BE algorithms.

Large discrepancies, already discussed in [22] and for factorial moments in [12], are seen for the model without BEC. Inclusion of BE-effects using the BE<sub>32</sub> algorithm leads to considerably better agreement, in particular in domains of  $y$ ,  $y \times \Phi$  and  $y \times \Phi \times \ln p_T$ . In  $\Phi$ , disagreements similar to those for like-sign multiplets are also seen here. In addition,  $K_2(\Phi)$  may be somewhat overestimated for large  $M$ .

To assess the sensitivity of the cumulants to variations in the BEC algorithms available in PYTHIA, we have further considered the algorithms BE <sub>$\lambda$</sub>  and BE<sub>0</sub> (see appendix).

Using the same parameter values as for BE<sub>32</sub>, we observe that BE <sub>$\lambda$</sub>  slightly underestimates  $K_2(y)$  and overestimates  $K_2(\Phi)$  for like-sign pairs (Fig. 3), whereas the results coincide with those from BE<sub>32</sub> in 2D and 3D. For all-charge multiplets (Figs. 4 and 5), the predicted cumulants generally fall below those for BE<sub>32</sub>, except for  $K_3$  and  $K_4$  in 2D and 3D, where the differences are small. We note, in particular, that the predicted  $K_2(y)$  (Fig. 4) essentially coincides with the PYTHIA results *without* BEC. The differences with respect to BE<sub>32</sub> are related to the different pair-correlation functions  $g_2(Q)$  (Eqs. 8 and 9 of the appendix) used in the algorithms. Although a different choice of the parameters  $R$  and  $\lambda$  may improve the agreement with the data, we have not attempted such fine-tuning.

In  $W$ -mass studies using the fully hadronic decay channel of the reaction  $e^+e^- \rightarrow W^+W^-$ , and assuming that pairs of pions from different  $W$ 's are fully affected by BEC, algorithm BE<sub>32</sub> is found to introduce a negative mass-shift, whereas BE <sub>$\lambda$</sub>  generates a positive shift [23]. The mass-shift occurs since the BE-induced momentum changes increase the likelihood that soft particles in an event are assigned to the wrong jet. This, in turn, depends on the strength of the particle correlations in 3D momentum space. Since BE<sub>32</sub> and BE <sub>$\lambda$</sub>  provide a reasonable description of the domain-size dependence of all-charge cumulants in 3D, both algorithms should be considered in  $WW$  studies.

Finally, we consider the model predictions based on the algorithm BE<sub>0</sub> (dash-dotted curves in the figures) for the same parameter values as quoted above. For like-sign pairs (Fig. 3),  $K_2(y)$  and especially  $K_2(\Phi)$  are overestimated. This is also the case for  $K_2(\Phi)$  for all-charge pairs shown in Fig. 4. In contrast, all-charge higher-order cumulants differ little from those obtained with BE<sub>32</sub>. It should be noted that the BE<sub>0</sub> algorithm, contrary to BE<sub>32</sub> and BE <sub>$\lambda$</sub> , enforces energy conservation by a global rescaling of all final-state hadron momenta. This procedure affects the full hadronic final state and induces a large artificial shift in the  $W$ -mass when applied to the reaction  $e^+e^- \rightarrow W^+W^- \rightarrow$  hadrons. It is, for that reason, disfavoured by the authors of [23].

Traditional studies of the Bose-Einstein effect most often consider only the second-order correlation function for like-sign particle pairs, which is measured as a function of  $Q^2$ , the square of the difference in four-momenta  $p_i$  ( $i = 1, 2$ ) of particles in the pair. The variable  $Q^2$  is related to the 3D cell-size used in this paper, via the approximate relation [33]:

$$Q^2 \approx m^2 \left[ \beta^2 \delta\Phi^2 + (1 + \beta^2) \delta y^2 + \frac{\beta^4 \delta x^2}{(1 + \beta)^2} \right], \quad (6)$$

---

<sup>7</sup>For a recent theoretical discussion of multi-boson BEC, see [32].

valid for small domains in  $y$ ,  $\Phi$  and  $\ln p_T$ . Here  $\beta = p_T/m$ ,  $m$  is the particle mass and  $\delta x = \ln(p_{T1}/p_{T2})$ . It follows that a small cell-size in 3D corresponds to small  $Q^2$ . The reverse is not true. Equation (6) implies that a measurement of  $K_2$  versus  $M$  in 3D is roughly equivalent to that of the inclusive two-particle  $Q$ -distribution.

As a check of the consistency of our results, we have compared predictions for the inclusive two-particle  $Q$ -distribution of like-sign pairs (single-particle rapidity restricted to the interval  $-2 \leq y \leq 2$ ) from the BE<sub>32</sub> model to that extracted from the data and fully corrected for detector effects. For the values of the BEC parameters  $R$  and  $\lambda$  quoted above, satisfactory agreement is obtained (not shown).

In recent work, several LEP experiments have analyzed the second-order like-sign correlation function in terms of individual components of the four-vector  $Q$  [16]. If interpreted as a measurement of the space-time extent of the particle emitting source, such results show that the emission volume has an elongated shape with respect to the event axis. The BE algorithms discussed here, which treat all components of  $Q$  symmetrically, are unable to reproduce these measurements [34]. It is therefore possible, although to be verified, that the measured anisotropy of the two-particle correlation function may be responsible for some of the PYTHIA model discrepancies, e.g. for 1D cumulants in  $\Phi$  domains, observed in the present analysis.

In summary, a comparison with PYTHIA predictions shows that short-range correlations of the BE-type are needed, at least in this model, to reproduce the magnitude and the  $\Delta$ -dependence of the cumulants for like-sign multiplets. This further leads to a much improved description of not only two-particle but also of higher-order correlations in all-charge multiplets. Since Bose-Einstein correlations are a well-established phenomenon in multiparticle production, it is likely that the above conclusion has wider validity than the model from which it was derived.

### 4.3 The Ochs-Wosiek relation for cumulants

The success of the PYTHIA model with BEC in predicting both the magnitude and domain-size dependence of cumulants, has led us to consider the inter-dependence of these quantities in more detail.

In Fig. 6 we plot  $K_3$  and  $K_4$  in 2D and 3D, for each value of  $M$  as a function of  $K_2$ . We observe that the 2D and 3D data for all-charge, as well as for like-sign multiplets follow approximately, within errors, the same functional dependence. The solid lines is a simple fit to the function

$$\ln K_q = a_q + r_q \ln K_2. \quad (7)$$

The fitted slope values are  $r_3 = 2.3$  and  $r_4 = 3.8$ . This is evidence that the slope  $r_q$  increases with the order of the cumulant. The  $q$ -dependence of the slopes is of particular interest in multiplicative cascade models of hadronisation, and indicative of the mechanism causing scale-invariant fluctuations [2, 35].

Figure 6 suggests that the *cumulants* of different orders obey simple so-called ‘‘hierarchical’’ relations, analogous to the Ochs-Wosiek relation, first established for *factorial moments* [36]. Interestingly, all-charge as well as like-sign multiplets are seen to follow, within errors, the same functional dependence. Hierarchical relations of similar type are commonly encountered, or conjectured, in various branches of many-body physics (see e.g. [5]), but a satisfactory explanation within particle production phenomenology or QCD remains to be found.



Simple relations among the cumulants of different orders exist for certain probability distributions, such as the Negative Binomial distribution, which often parameterizes successfully the multiplicity distribution of hadrons in restricted phase space regions [37]. For this distribution, one has  $K_q = (q - 1)! K_2^{q-1}$  ( $q = 3, 4, \dots$ ), showing that the cumulants are here solely determined by  $K_2$ . This relation is shown in Fig. 6 (dashed line). Comparing to the data, we conclude that the multiplicity distribution of all charged particles, as well as that of like-sign particles, deviates strongly from a Negative Binomial in small phase space domains. For further discussion, in the present context, of this and other much studied multiplicity distributions we refer to [38].

The Ochs-Wosiek type of relation exhibited by the data in Fig. 6 may explain why the BE algorithms in PYTHIA generate higher-order correlations of (approximately) the correct magnitude. Assuming that the hadronization dynamics is such that higher-order correlation functions can be constructed from second-order correlations only, methods that are designed to ensure agreement with the two-particle correlation function, could then automatically generate higher-order ones of the correct magnitude.

## 5 Summary and conclusions

In this paper we have presented a comparative study of like-sign and all-charge genuine correlations between two and more hadrons produced in  $e^+e^-$  annihilation at the  $Z^0$  energy. The high-statistics data on hadronic  $Z^0$  decays recorded with the OPAL detector from 1991 through 1995 were used to measure normalized factorial cumulants as a function of the domain size,  $\Delta$ , in  $D$ -dimensional domains ( $D = 1, 2, 3$ ) in rapidity, azimuthal angle and (the logarithm of) transverse momentum, defined in the event sphericity frame.

Both all-charge and like-sign multiplets show strong positive genuine correlations up to fourth order. They are stronger in rapidity than in azimuthal angle. One-dimensional cumulants initially increase rapidly with decreasing size of the phase space cells but saturate rather quickly. In contrast, 2D and especially 3D cumulants continue to increase and exhibit intermittency-like behaviour.

Comparing all-charge and like-sign multiplets in 2D and 3D phase space cells, we observe that the rise of the cumulants for all-charge multiplets is increasingly driven by that of like-sign multiplets as  $\Delta$  becomes smaller. This points to the likely influence of Bose-Einstein correlations.

The 2D and 3D cumulants  $K_3$  and  $K_4$ , considered as a function of  $K_2$ , follow approximately a linear relation of the Ochs-Wosiek type:  $\ln K_q \sim \ln K_2$ , independent of  $D$  and the same for all-charge and for like-sign particle groups. This suggests that, for a given domain  $\Delta$ , correlation functions of different orders are not independent but determined, to a large extent, by two-particle correlations.

The data have been compared with predictions from the Monte Carlo event generator PYTHIA, previously tuned to single-particle and event-shape OPAL data. The model describes well dynamical fluctuations in large phase space domains, *e.g.* caused by jet production, and shorter-range correlations attributable to resonance decays. However, the results of this paper, together with earlier less precise data, show that these ingredients alone are insufficient to explain the magnitude and domain-size dependence of the factorial cumulants. To achieve a



more satisfactory data description, short-range correlations of the Bose-Einstein type between identical particles need to be included.

The importance of BE-type effects has been studied using algorithms implemented in PYTHIA. We find that the model  $BE_{32}$  is able to simultaneously account for the magnitude and  $\Delta$ -dependence of like-sign as well as of all-charge cumulants. Other models,  $BE_0$  and  $BE_\lambda$ , when using the same parameters as for  $BE_{32}$ , provide also a reasonable description of the data. Although the algorithms implement pair-wise BEC only, surprisingly good agreement with the measured third- and fourth-order cumulants is observed. This could be a consequence of the Ochs-Wosiek type of inter-relationship between cumulants of different orders, exhibited by the data.

#### Acknowledgements:

We particularly wish to thank the SL Division for the efficient operation of the LEP accelerator at all energies and for their close cooperation with our experimental group. We thank our colleagues from CEA, DAPNIA/SPP, CE-Saclay for their efforts over the years on the time-of-flight and trigger systems which we continue to use. In addition to the support staff at our own institutions we are pleased to acknowledge the  
Department of Energy, USA,  
National Science Foundation, USA,  
Particle Physics and Astronomy Research Council, UK,  
Natural Sciences and Engineering Research Council, Canada,  
Israel Science Foundation, administered by the Israel Academy of Science and Humanities,  
Minerva Gesellschaft,  
Benozziyo Center for High Energy Physics,  
Japanese Ministry of Education, Science and Culture (the Monbusho) and a grant under the Monbusho International Science Research Program,  
Japanese Society for the Promotion of Science (JSPS),  
German Israeli Bi-national Science Foundation (GIF),  
Bundesministerium für Bildung und Forschung, Germany,  
National Research Council of Canada,  
Research Corporation, USA,  
Hungarian Foundation for Scientific Research, OTKA T-029328, T023793 and OTKA F-023259.

## Appendix: Modelling BEC in PYTHIA

As emphasized in [23], no rigorous method exists to date which would allow to account for the Bose-Einstein symmetrization of the production amplitudes in Monte Carlo event generators. The algorithms implemented in the Monte Carlo event generator PYTHIA [24] which simulate the BE effect, are all based on introducing BEC as local shifts of final-state particle momenta among pairs of identical particles. They differ only in the way global energy and momentum conservation is ensured. Other, so-called “global-weight” methods, have been proposed wherein a single weight-factor is assigned to each event, calculated on the basis of a model for the identical-pair two-particle correlation function [39, 40].

The PYTHIA algorithms take the hadrons produced by the string fragmentation, where no BE effects are present, and shift the momenta of mesons  $i$  and  $j$  such that the inclusive distribution of the relative separation  $Q$  of identical pairs is enhanced by a factor  $g_2(Q) \geq 1$ . The latter, as used here, is parameterized with the phenomenological form<sup>8</sup>

$$g_2(Q) = 1 + \lambda e^{-R^2 Q^2}, \quad (8)$$

where  $Q$  is the difference in four-momenta of the pair,  $Q^2 = -(p_1 - p_2)^2$ .

Short-lived resonances like the  $\rho$  and  $K^*$  are allowed to decay before the BE procedure is applied, while decay products of longer-lived ones (width  $\Gamma < 20$  MeV/ $c^2$ ) are not affected. The procedure also influences groups of non-identical particles causing e.g. a shift of the  $\rho^0$  mass peak [15, 41].

In this paper we compare the data to simulations based on the PYTHIA algorithms  $BE_0$ ,  $BE_{32}$  and  $BE_\lambda$ , following the nomenclature in [23].

*In the  $BE_0$  algorithm*, momentum is conserved exactly, but energy conservation is explicitly broken in the treatment of individual particle pairs. It is restored only by a global rescaling of all final-state hadron momenta, thus affecting the full hadronic final state.

The other algorithms avoid global energy rescaling by introducing additional momentum shifts for some pairs of particles,  $(k, l)$ , not necessarily identical, in a local region around each identical pair  $(i, j)$ .

*The algorithm  $BE_{32}$* , which is applied to identical pairs only, is based on the ansatz

$$g_2(Q) = \{1 + \lambda \exp(-Q^2 R^2)\} \{1 + \alpha \lambda \exp(-Q^2 R^2/9) (1 - \exp(-Q^2 R^2/4))\}, \quad (9)$$

( $\alpha$  is an adjustable parameter) which attempts to mimic effects due to oscillations below and above unity of the pair-weights, as found in some models [39].

*In the algorithm  $BE_\lambda$* , the form (8) of  $g_2(Q)$  is retained. For each pair of identical particles  $(i, j)$ , a pair of non-identical particles,  $(k, l)$ , neither identical to  $i$  or  $j$ , is found close to  $(i, j)$ . For each momentum shift among particles  $i$  and  $j$ , a corresponding shift among the particles  $k$  and  $l$  is found so that the total energy and momentum in the  $i, j, k, l$  system is conserved. As a measure of “closeness”,  $BE_\lambda$  uses the so-called  $\lambda$ -measure [42], related to the string length in the Lund string fragmentation framework.

A given particle is likely to belong to several identical pairs in an event. The net shift in particle momenta and energies therefore depends on the complete configuration of all identical

---

<sup>8</sup>In naive BE models, based on the analogy with optics and assuming a *static* incoherent emission source,  $R$  is related to the size of the source;  $\lambda$  quantifies the strength of the BE effect.

particles. This introduces complex effects, not only among identical pairs but also among unlike-sign pairs and higher multiplicity multiplets of nearby particles. As a result, genuine higher-order correlations emerge. For a full description of the BE algorithms mentioned above, ref. [23] should be consulted.

## References

- [1] E.A. De Wolf, I.M. Dremin and W. Kittel, Phys. Rep. **270** (1996) 1.
- [2] A. Białaś and R. Peschanski, Nucl. Phys. **B 273** (1986) 703.
- [3] M.G. Kendall and A. Stuart, *The Advanced Theory of Statistics*, Vol. 1, C. Griffin and Co., London 1969.
- [4] A.H. Mueller, Phys. Rev. **D 4** (1971) 150.
- [5] P. Carruthers and I. Sarcevic, Phys. Rev. Lett. **63** (1989) 1562;  
E.A. De Wolf, Acta Phys. Pol. **B 21** (1990) 611.
- [6] P. Bożek, M. Płoszajczak and R. Botet, Phys. Rep. **252** (1995) 101.
- [7] B. Buschbeck, H.C. Eggers and P. Lipa, Phys. Lett. **B 481** (2000) 187;  
G. Alexander and E.K.G. Sarkisyan, Phys. Lett. **B 487** (2000) 215;  
M.A. Braun, F. del Moral and C. Pajares, Eur. Phys. J. **C 21** (2001).
- [8] M. Gyulassy, Festschrift L. Van Hove, eds. A. Giovannini and W. Kittel (World Scientific, Singapore, 1990) p.479.
- [9] R. Hanbury Brown and R.Q. Twiss, Phil. Mag. **54** (1954) 633;  
R. Hanbury Brown and R.Q. Twiss, Nature **178** (1956) 1046, 1447.
- [10] G. Goldhaber, S. Goldhaber, W. Lee and A. Pais, Phys. Rev. **120** (1960) 300;  
E.V. Shuryak, Phys. Lett. **44B** (1973) 387;  
G. Cocconi, Phys. Lett. **49B** (1974) 459.
- [11] R.M. Weiner, Phys. Rep. **327** (2000) 249.
- [12] I. Derado, G. Jancso and N. Schmitz, Z. Phys. **C 56** (1992) 553;  
NA22 Collaboration, N. Agababyan *et al.*, Z. Phys. **C 59** (1993) 405;  
UA1-MB Collaboration, N. Neumeister *et al.*, Z. Phys. **C 60** (1993) 633;  
E665 Collaboration, M.R. Adams *et al.*, Phys. Lett. **B 335** (1994) 535;  
NA35 Collaboration, J. Bächler *et al.*, Z. Phys. **C 61** (1994) 551.
- [13] DELPHI Collaboration, P. Abreu *et al.*, Phys. Lett. **B 355** (1995) 415;  
OPAL Collaboration, K. Ackerstaff *et al.*, Eur. Phys. J. **C 5** (1998) 239.
- [14] OPAL Collaboration, P.D. Acton *et al.*, Phys. Lett. **B 267** (1991) 143;  
ALEPH Collaboration, D. Decamp *et al.*, Z. Phys. **C 54** (1992) 75;  
DELPHI Collaboration, P. Abreu *et al.*, Phys. Lett. **B 286** (1992) 291;  
OPAL Collaboration, P.D. Acton *et al.*, Phys. Lett. **B 298** (1993) 456;  
DELPHI Collaboration, P. Abreu *et al.*, Phys. Lett. **B 323** (1994) 242;  
OPAL Collaboration, R. Akers *et al.*, Z. Phys. **C 67** (1995) 389;  
OPAL Collaboration, G. Alexander *et al.*, Z. Phys. **C 72** (1996) 389;  
DELPHI Collaboration, P. Abreu *et al.*, Phys. Lett. **B 379** (1996) 330.

- [15] DELPHI Collaboration, P. Abreu *et al.*, Z. Phys. **C 63** (1994) 17.
- [16] L3 Collaboration, M. Acciarri *et al.*, Phys. Lett. **B 458** (1999) 517;  
DELPHI Collaboration, P. Abreu *et al.*, Phys. Lett. **B 471** (2000) 460;  
OPAL Collaboration, G. Abbiendi *et al.*, Eur. Phys. J. **C 16** (2000) 423.
- [17] NA22 Collaboration, N.M. Agababyan *et al.*, Z. Phys. **C 68** (1995) 229;  
WA98 Collaboration, M.M. Aggarwal *et al.*, Phys. Rev. Lett. **85** (2000) 2895;  
NA44 Collaboration, I.G. Bearden *et al.*, Phys. Lett. **B 517** (2001) 25.
- [18] L. Lönnblad and T. Sjöstrand, Phys. Lett. **B 351** (1995) 293.
- [19] V.A. Khoze and T. Sjöstrand, Eur. Phys. J. **C 6** (1999) 271.
- [20] Z. Kunszt *et al.*, in “Physics at LEP2”, eds. G. Altarelli, T. Sjöstrand and F. Zwirner, CERN Report 96-01, Vol.1 (1996), p. 141.
- [21] DELPHI Collaboration, P. Abreu *et al.*, Phys. Lett. **B 401** (1997) 181;  
OPAL Collaboration, G. Abbiendi *et al.*, Eur. Phys. J. **C 8** (1999) 559;  
ALEPH Collaboration, R. Barate *et al.*, Phys. Lett. **B 478** (2000) 50;  
L3 Collaboration, M. Acciarri *et al.*, Phys. Lett. **B 493** (2000) 233;  
For recent reviews see: W. Kittel, *Interconnection Effects and  $W^+W^-$  decays*, Proc. XXXIVth Rencontres de Moriond, QCD and High Energy Interactions, Les Arcs (France), Nijmegen preprint HEN-420 (1999) [[hep-ph/9905394](#)];  
N. van Remortel, *Bose-Einstein correlations in  $WW$  events at LEP*, Proc. XXXVI Rencontres de Moriond, QCD and High Energy Interactions, Les Arcs (France), [hep-ex/0104011](#);  
O. Pooth, *Bose-Einstein correlations in  $W$ -pair events*, Proc. Int. Europhysics Conf. on High Energy Physics, Budapest (Hungary) 2001, J. High Energy Phys., Conf. Proc., PRHEP-hep 2001/120.
- [22] OPAL Collaboration, G. Abbiendi *et al.*, Eur. Phys. J. **C 11** (1999) 239.
- [23] L. Lönnblad and T. Sjöstrand, Eur. Phys. J. **C 2** (1998) 165.
- [24] T. Sjöstrand, Comp. Phys. Comm. **82** (1994) 74;  
T. Sjöstrand *et al.*, Comp. Phys. Comm. **135** (2001) 238.
- [25] K. Kadija and P. Seyboth, Z. Phys. **C 61** (1994) 465.
- [26] OPAL Collaboration, K. Ahmet *et al.*, Nucl. Instr. Meth. **A 305** (1991) 275;  
O. Biebel *et al.*, Nucl. Instr. Meth. **A 323** (1992) 169;  
P.P. Allport *et al.*, Nucl. Instr. Meth. **A 324** (1993) 34;  
P.P. Allport *et al.*, Nucl. Instr. Meth. **A 346** (1994) 476.
- [27] M. Hauschild *et al.*, Nucl. Instr. Meth. **A 314** (1992) 174.
- [28] J. Allison *et al.*, Nucl. Instr. Meth. **A 317** (1992) 47.
- [29] OPAL Collaboration, G. Alexander *et al.*, Z. Phys. **C69** (1996) 543.

- [30] OPAL Collaboration, P. D. Acton *et al.*, Z. Phys. **C 58** (1993) 387;  
OPAL Collaboration, M. Z. Akrawy *et al.*, Z. Phys. **C 47** (1990) 505.
- [31] I.V. Andreev *et al.*, Int. J. Mod. Phys. **A 10** (1995) 3951.
- [32] U. Heinz, P. Scotto and Q.H. Zhang, Ann. of Phys. (N.Y.) **288** (2001) 325.
- [33] K. Fiałkowski, Proc. 24th Int. Symp. Multiparticle Dynamics, Vietri sul Mare (Italy) 1994,  
Eds. A. Giovannini *et al.* (World Scientific, Singapore, 1995), p. 104.
- [34] K. Fiałkowski and R. Wit, Acta Phys. Pol. **B 32** (2001) 1233.
- [35] Ph. Brax and R. Peschanski, Phys. Lett. **B 253** (1991) 225.
- [36] W. Ochs and J. Wosiek, Phys. Lett. **B 214** (1988) 617;  
W. Ochs, Z. Phys. **C 50** (1991) 339.
- [37] For reviews see P. Carruthers and C.C. Shi, Int. J. Mod. Phys. **A 2** (1987) 1447;  
G. Giacomelli, Int. J. Mod. Phys. **A 5** (1990) 223.
- [38] E.K.G. Sarkisyan, Phys. Lett. **B 477** (2000) 1.
- [39] B. Andersson and M. Ringnér, Nucl. Phys. **B 513** (1998) 627;  
B. Andersson and M. Ringnér, Phys. Lett. **B 421** (1998) 283;  
J. Hakkinen and M. Ringnér, Eur. Phys. J. **C 5** (1998) 275.
- [40] A. Białas and A. Krzywicki, Phys. Lett. **B 354** (1995) 134;  
T. Wibig, Phys. Rev. **D 53** (1996) 3586;  
S. Jadach and K. Zalewski, Acta Phys. Pol. **B28** (1997) 1363;  
K. Fiałkowski and R. Wit, Eur. Phys. J. **C 13** (2000) 133;  
V. Kartvelishvili and R. Kvatadze, Phys. Lett. **B 514** (2001) 7.
- [41] OPAL Collaboration, P.D. Acton *et al.*, Z. Phys. **C 56** (1992) 521;  
G.D. Lafferty, Z. Phys. **C 60** (1993) 659;  
DELPHI Collaboration, P. Abreu *et al.*, Z. Phys. **C 65** (1995) 587;  
ALEPH Collaboration, D. Buskulic *et al.*, Z. Phys. **C 69** (1996) 379 .
- [42] B. Andersson, P. Dahlqvist and G. Gustafson, Z. Phys. **C 44** (1989) 455;  
B. Andersson, G. Gustafson, A. Nilsson and C. Sjögren, Z. Phys. **C 49** (1991) 79.



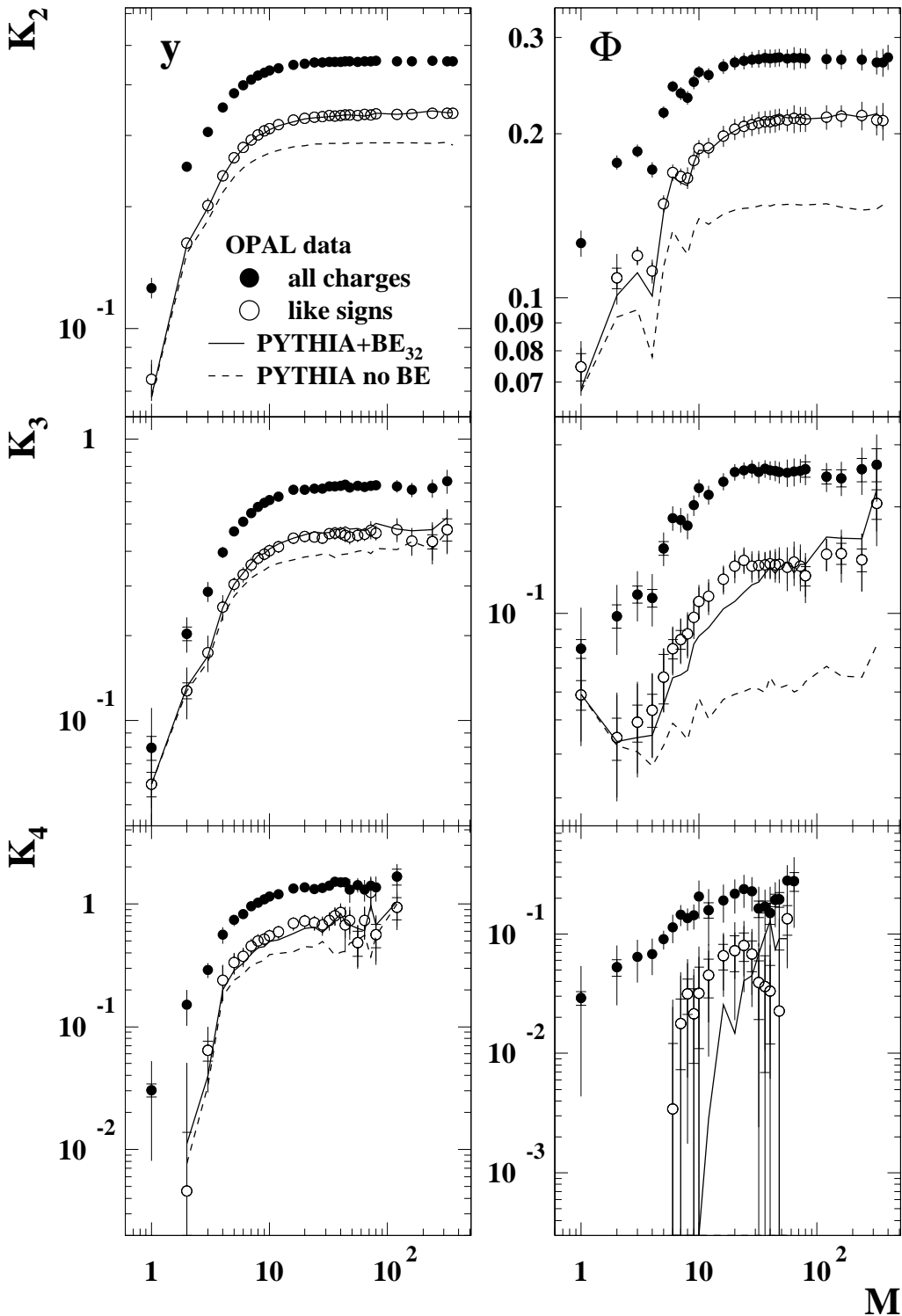


Figure 1: The cumulants  $K_q$  in one-dimensional domains of rapidity ( $y$ ) and azimuthal angle ( $\Phi$ ) for all charged hadrons (solid symbols) and for multiplets of like-sign particles (open symbols), versus  $M$ . Where two error-bars are shown, inner ones are statistical, and outer ones are statistical and systematic errors added in quadrature. The lines connect Monte Carlo predictions for like sign cumulants from PYTHIA without BEC (dashed) and with BEC (full) simulated with algorithm BE<sub>32</sub> [23] (see text).

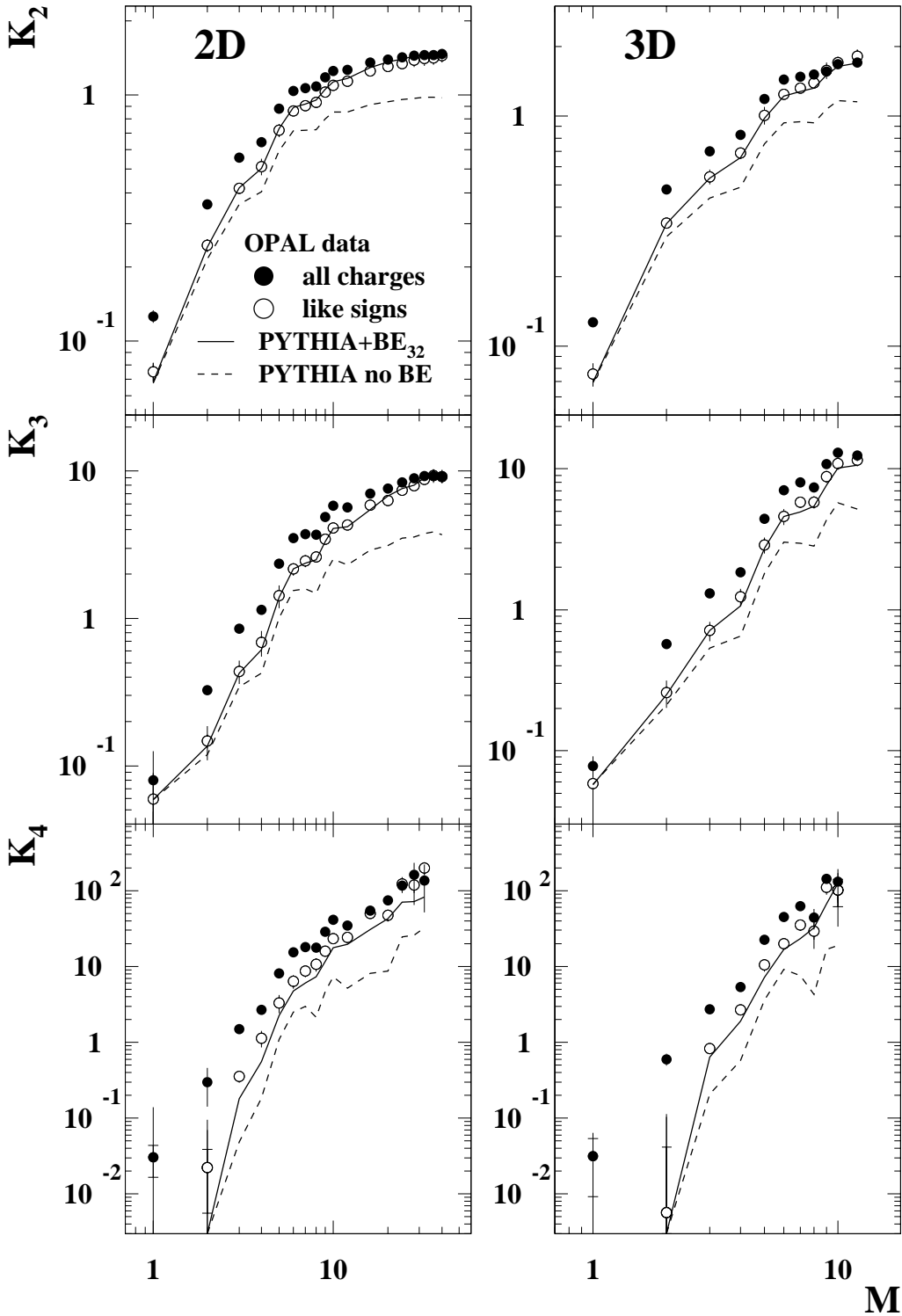


Figure 2: *The cumulants  $K_q$  in two-dimensional  $\Delta y \times \Delta \Phi$  (2D) and three-dimensional  $\Delta y \times \Delta \Phi \times \Delta \ln p_T$  (3D) domains for all charged hadrons (solid symbols) and for multiplets of like-sign particles (open symbols), versus  $M$ . Where two error-bars are shown, inner ones are statistical, and outer ones are statistical and systematic errors added in quadrature. The lines connect Monte Carlo predictions from PYTHIA without BEC (dashed) and with BEC simulated with algorithm  $BE_{32}$  [23] (see text).*

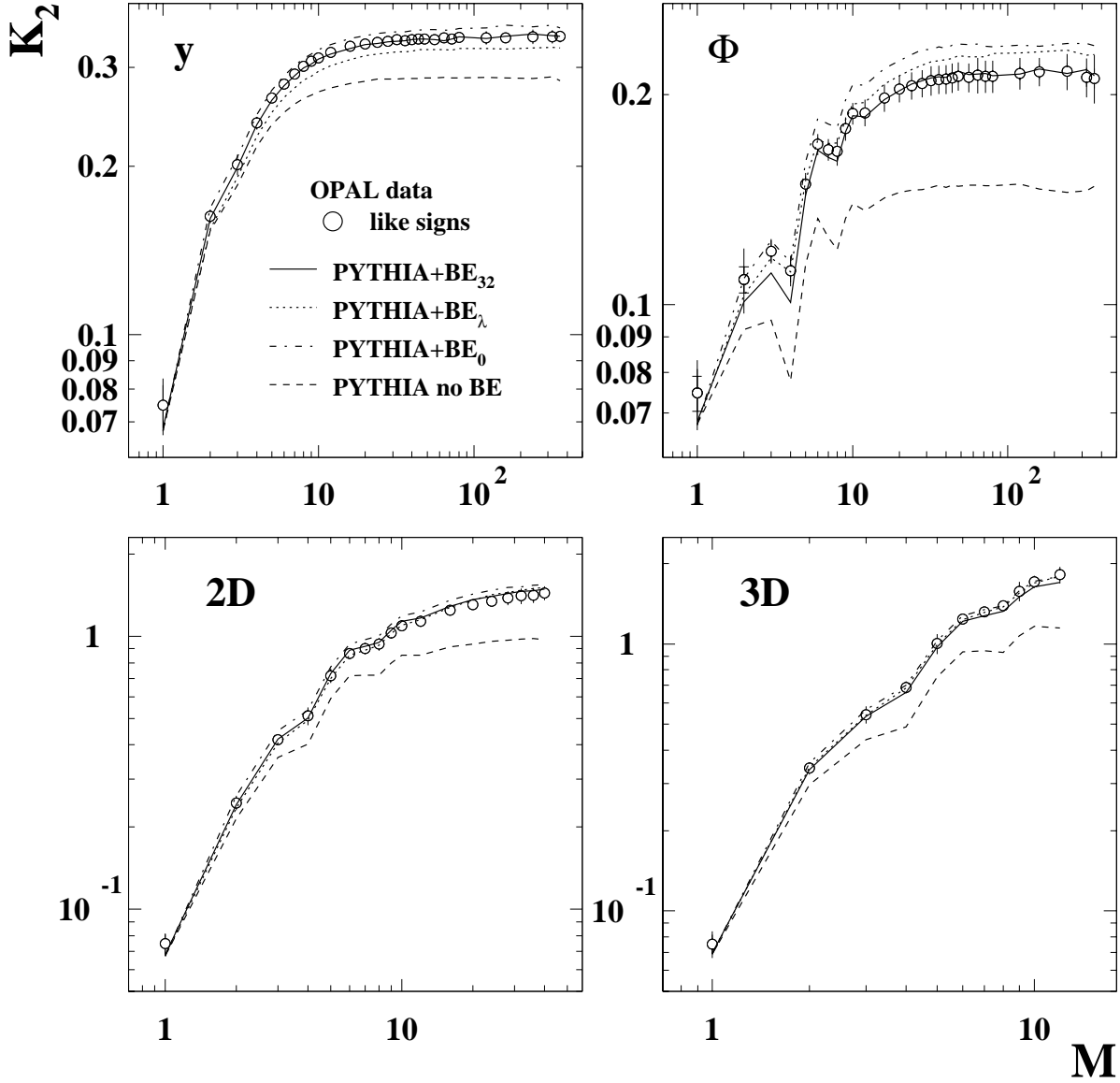


Figure 3: The cumulants  $K_2$  for like-sign pairs in one-dimensional domains of rapidity ( $y$ ) and azimuthal angle ( $\Phi$ ), and in two-dimensional  $\Delta y \times \Delta \Phi$  (2D) and three-dimensional  $\Delta y \times \Delta \Phi \times \Delta \ln p_T$  (3D) domains versus  $M$ . The error-bars show statistical and systematic errors added in quadrature. The lines connect Monte Carlo predictions from PYTHIA, without BEC and with various Bose-Einstein algorithms [23] (see text).

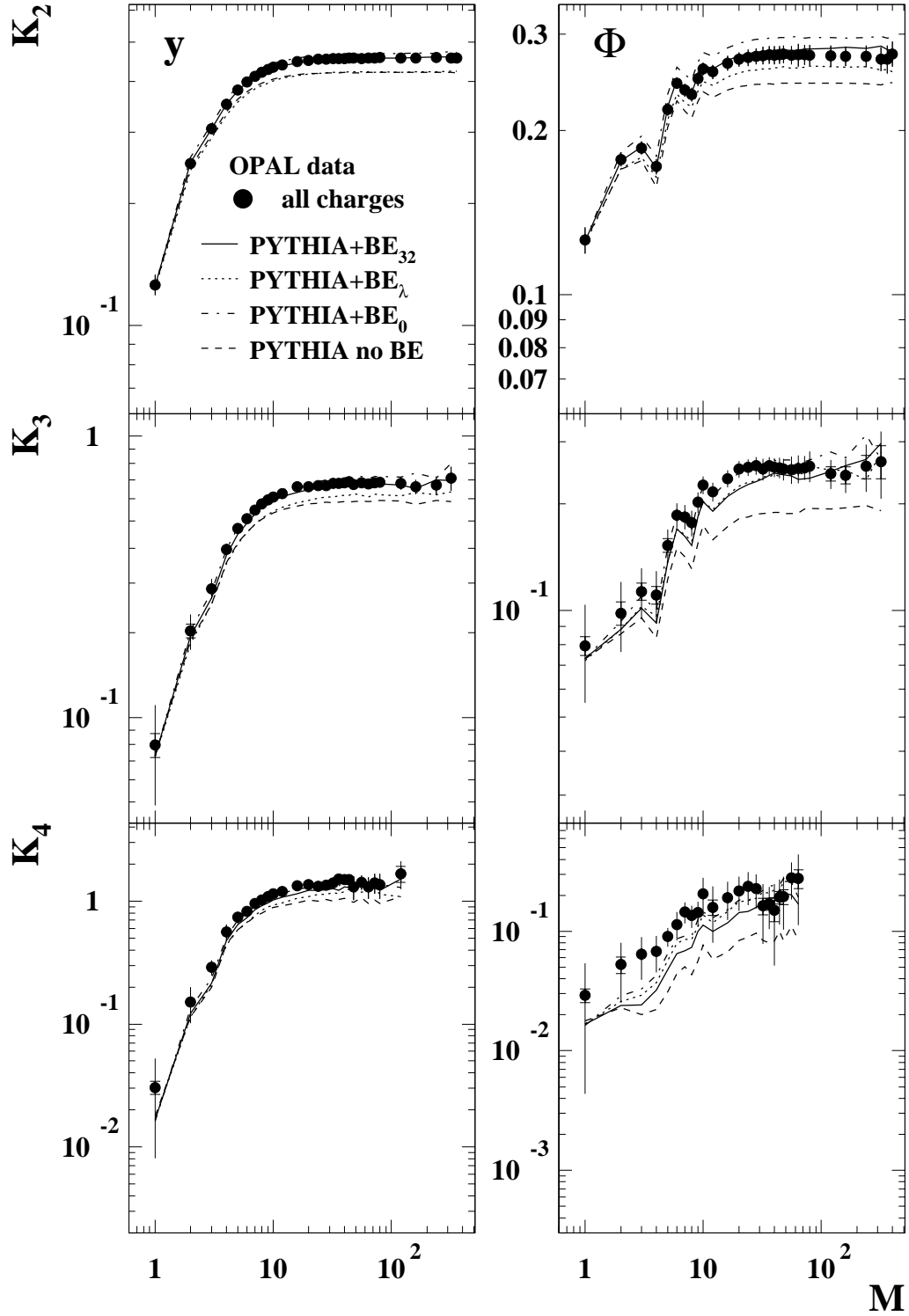


Figure 4: The cumulants  $K_q$  in one-dimensional domains of rapidity ( $y$ ) and azimuthal angle ( $\Phi$ ) for all charged hadrons, as in Fig. 1, versus  $M$ . Where two error-bars are shown, inner ones are statistical, and outer ones are statistical and systematic errors added in quadrature. The lines connect Monte Carlo predictions from PYTHIA, without BEC and with various Bose-Einstein algorithms [23] (see text).

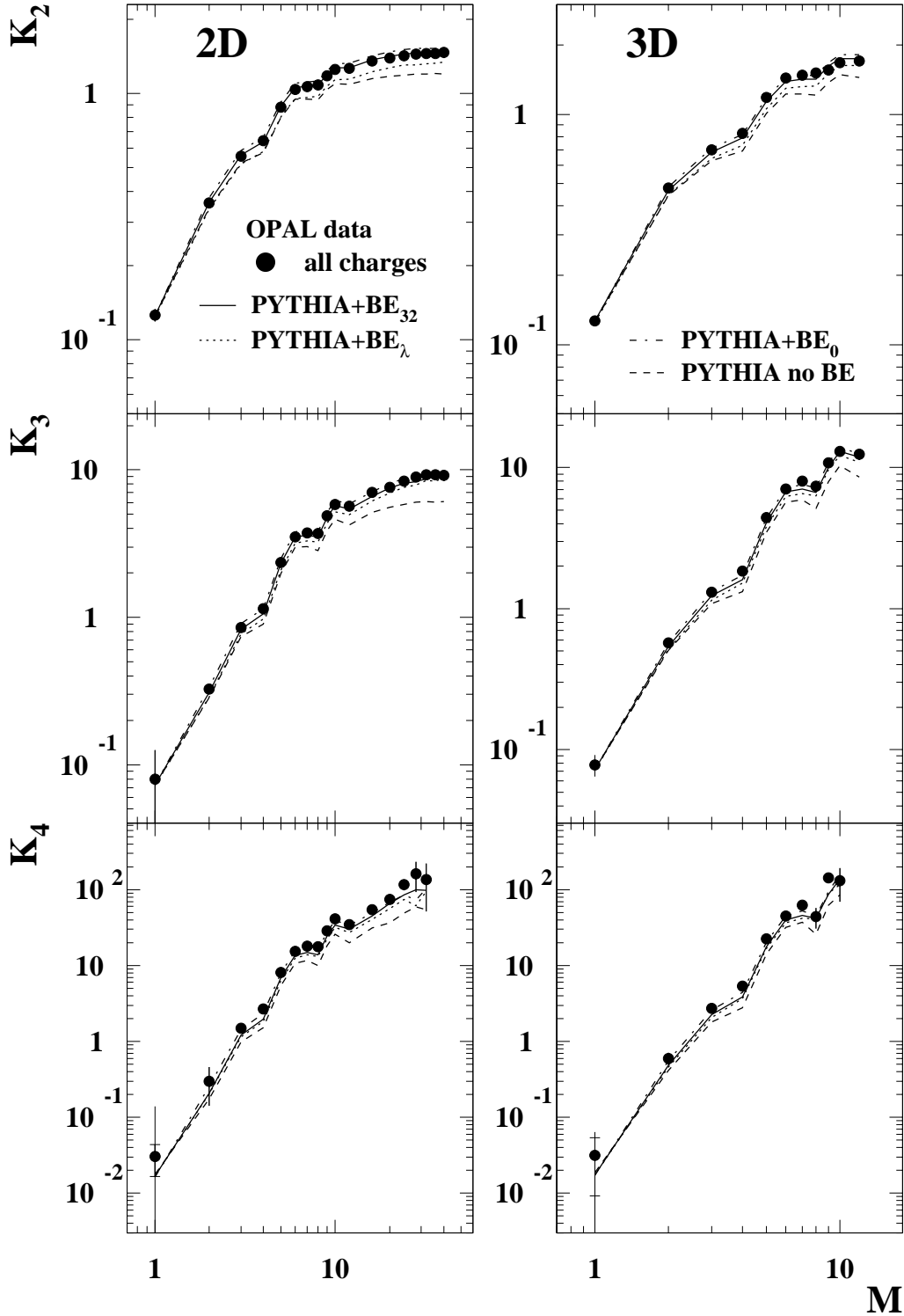


Figure 5: The cumulants  $K_q$  in two-dimensional  $\Delta y \times \Delta \Phi$  (2D) and three-dimensional  $\Delta y \times \Delta \Phi \times \Delta \ln p_T$  (3D) domains for all charged hadrons as in Fig. 2, versus  $M$ . Where two error bars are shown, inner ones are statistical, and outer ones are statistical and systematic errors added in quadrature. The lines connect Monte Carlo predictions from PYTHIA, without BEC and with various Bose-Einstein algorithms [23] (see text).

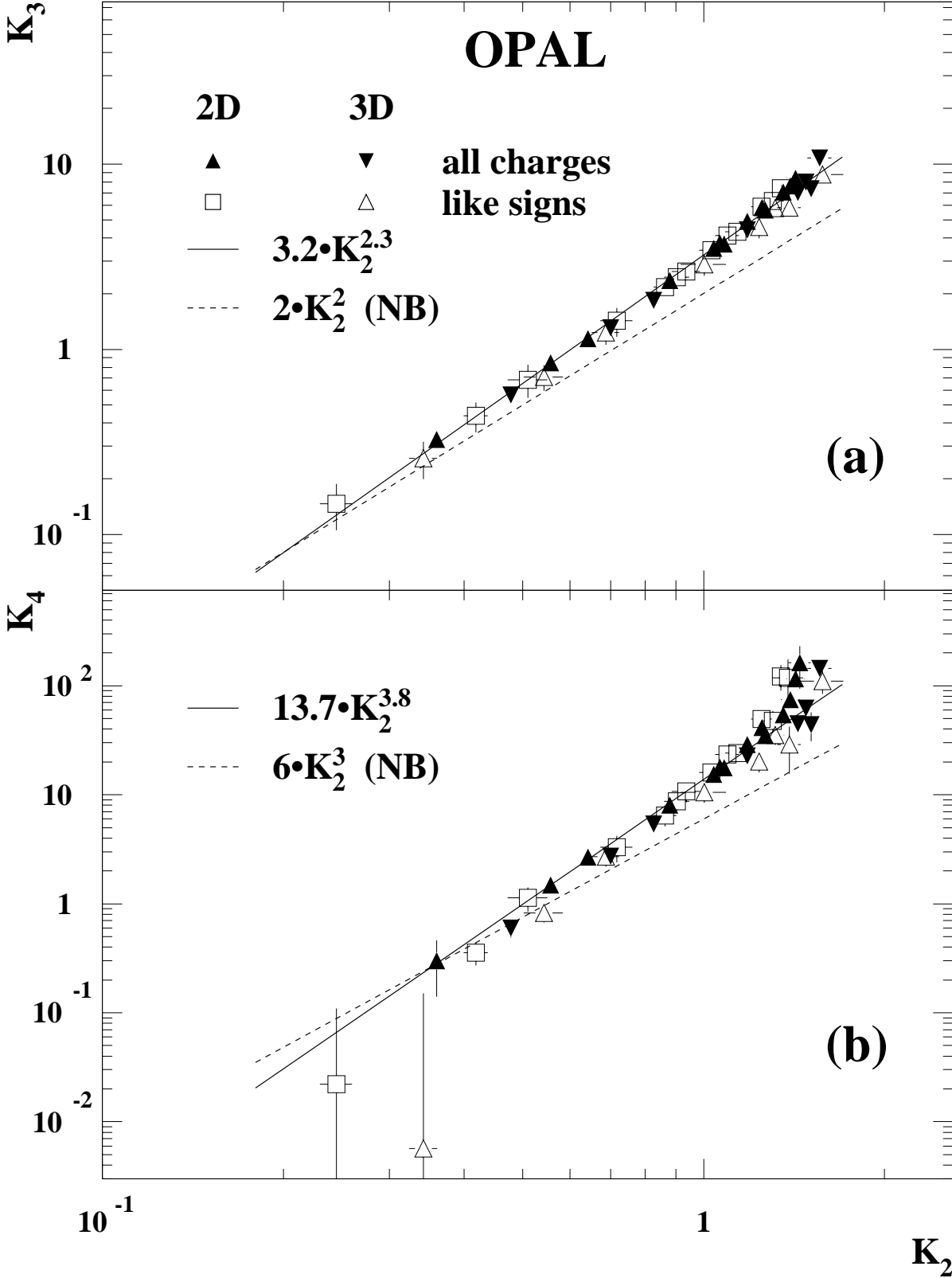


Figure 6: The Ochs-Wosiek plot in two-dimensional  $\Delta y \times \Delta \Phi$  (2D) and three-dimensional  $\Delta y \times \Delta \Phi \times \Delta \ln p_T$  (3D) domains for all charged hadrons (solid symbols) and for multiplets of like-sign particles (open symbols). The dashed line shows the function,  $K_q = (q - 1)! K_2^{q-1}$  ( $q = 3, 4$ ), valid for a Negative Binomial multiplicity distribution (NB) in each phase space cell. The solid line shows a fit with Eq. (7).